Available online at www.sciencedirect.com
SCIENCE DIRECT®
Journal of Power Sources 115 (2003) 1–11
JOURNAL OF POWER SOURCES
www.elsevier.com/locate/jpowsour

Corrosion resistance of 316L stainless steel with surface layer of Ni_2Al_3 or NiAl in molten carbonates

Youngjoon Moon*, Dokyol Lee

Division of Materials Science and Engineering, Korea University, 5-1 Anam-Dong, Sungbuk-Ku, Seoul 136-701, South Korea

Received 13 May 2002; received in revised form 21 July 2002; accepted 30 July 2002

Abstract

Double layers of nickel and aluminum are electroplated on a 316L stainless steel (316L SS) plate, which is routinely used as a separator in molten carbonate fuel cell (MCFC) stacks, and then heat-treated at 650 or 800 °C for 1 h. This results in the respective formation of a surface layer of Ni_2Al_3 or NiAl intermetallic compound, which are known to be highly corrosion-resistant in molten carbonate electrolyte. The corrosion behaviour of each plate in a molten electrolyte of $(Li_{0.62}K_{0.38})_2CO_3$ or $(Li_{0.52}Na_{0.48})_2CO_3$ is evaluated through immersion tests and polarisation measurements. The surface layer of Ni_2Al_3 or NiAl maintains good adhesion to the stainless steel substrate and no corrosion product is detected in any of the plates with a surface layer after immersion tests. Polarisation measurements reveal that, regardless of experimental conditions, the corrosion potentials of the plates with a surface layer shift to more positive values and the passive currents are lower than that for a bare SS plate. The corrosion rate of the NiAl surface layer is slightly lower than that of Ni_2Al_3.

Keywords: Corrosion resistance; Intermetallic compound; Corrosion potential; Critical anodic current density; Molten carbonate fuel cell

1. Introduction

It is now generally agreed that a molten carbonate fuel cell (MCFC) should be operated for over 40 000 h to compete with other power-generation systems on economic grounds. There still remain, however, many obstacles to this goal of lifetime, and corrosion of the separator plate is one of them. Many different alloys, for example Ni–base alloys or high chromium ferritic stainless steels, have been examined as the material for separators by various developers [1–6]. The Ni–base alloys have acceptable corrosion resistance, but are inadequate for practical use because of their high cost. The ferritic stainless steels, though relatively cheap, do not show sufficient corrosion resistance. Under anodic conditions, chromium in these steels forms an oxide scale of $LiCrO_2$ that is porous and non-protective [7]. After all these trials, Fe–Cr–Ni austenitic stainless steels (for example, 316L SS) have now become the most preferred material for the separator and their corrosion behaviour in the most frequently used electrolyte, viz. $(Li_{0.62}K_{0.38})_2CO_3$, is under intensive study. The austenitic stainless steel itself is not, however, a perfect material for the separator, especially the part in the wet seal area. This is because the oxide scales of Fe_3O_4 and FeO are produced in the area during MCFC operation, which induce the loss of electrolyte in the course of transformation to $LiFeO_2$. Therefore, it is a common practice that a corrosion-protective layer is formed on the surface of the 316L SS separator before use.

As mentioned above, $(Li_{0.62}K_{0.38})_2CO_3$ has so far been the popular choice of electrolyte for MCFCs. Recently, however, $(Li_{0.52}Na_{0.48})_2CO_3$ has attracted increasing attention due to its superior performance with respect to NiO cathode dissolution, electrolyte creepage and volatilisation, as well as ionic conductivity. Nevertheless, there have been only a few reports of the corrosion behaviour of 316L SS in $(Li_{0.52}Na_{0.48})_2CO_3$ [4,8].

In this study, a corrosion-protective surface layer of Ni_2Al_3 or NiAl intermetallic compound is formed on a 316L SS plate by electroplating of elemental metals and subsequent heat treatment at an appropriate temperature. The corrosion behaviour of the plates in an electrolyte of $(Li_{0.62}K_{0.38})_2CO_3$ or $(Li_{0.52}Na_{0.48})_2CO_3$ (called, respectively, Li/K or Li/Na hereafter) is studied through immersion tests and polarisation measurements.

* Corresponding author. Tel.: +82-2-3290-3707; fax: +82-2-928-3584.
E-mail address: yjmoon1971@yahoo.co.kr (Y. Moon).

0378-7753/02/$ – see front matter
PII: S0378-7753(02)00417-2

2. Experimental procedure

The surface layer of Ni_2Al_3 or NiAl intermetallic compound was formed on a 316L SS plate via the procedure shown in Fig. 1. A SS substrate of thickness 1 mm and area 15 mm × 7 mm was polished to a mirror finish with an aqueous slurry of 0.05 μm alumina, degreased with acetone, and dried. It was then pickled for 10 min in 10% HCl–10% H_2SO_4 aqueous solution at 60 °C and for a further 10 min in 10% HNO_3–10% HF aqueous solution at 25 °C. Nickel plating was carried out in a conventional Watt's bath [9] and preceded by nickel striking for better adhesion of the nickel layer to the substrate. Heat treatment was, however, necessary for full guarantee of adhesion and was performed at 1100 °C for 1 h in an argon atmosphere. Aluminum plating was carried out in an argon-filled glove box using a room temperature electroplated aluminum (REAL) process. In this process, the bath was prepared by adding $AlCl_3$ (Aldrich, 99.99%) to a tetra hydrofuran (Aldrich, 99.9%) solution saturated with $LiAlH_4$ (Aldrich, 95%), and stirring the solution for about a day to achieve homogeneous mixing. A 1.2 mm thick aluminum (High Purity Chemicals, 99.99%) plate, cut in the same size as the substrate, was used as the anode and a potential was applied across the cell using a dc power supply (HP E3617A). The thicknesses of the electroplated Ni and Al layers were 5 and 10 μm, respectively.

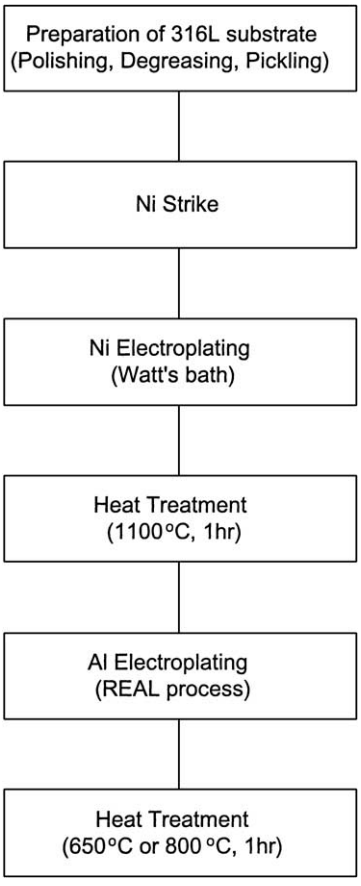

Fig. 1. Experimental procedure for sample preparation.

The Ni–Al electroplated plate was then heat-treated at an appropriate temperature in the range 600–950 °C for 1 h in an argon atmosphere so that a single phase of Ni_2Al_3 or NiAl could be formed by interdiffusion of Ni and Al.

The plate was characterised by means of X-ray diffraction (XRD, Rigaku Geigerflex DMAX-II A) to identify the phase of the surface layer, and a field emission-scanning electron microscope (FE-SEM, Hitachi 6300) or an energy-dispersive X-ray spectrometer (EDX, Oxford), respectively, to observe the morphology of its cross-section or to analyse the composition. The corrosion behaviour of the plate was investigated through immersion tests and electrochemical tests. For an immersion test, a plate was placed in an alumina crucible filled with the Li–K or Li–Na electrolyte and heated at 650 °C for 100 h. The electrolyte was prepared from well-dried Li_2CO_3, Na_2CO_3 and K_2CO_3 powders of reagent grade (Aldrich). The carbonate powders of an appropriate composition were mixed in a dry ball-mill for a day before use. The electrochemical test was also performed at 650 °C in a pot cell constructed, shown in Fig. 2. The Li–K or La–Na electrolyte was contained in an alumina crucible which was

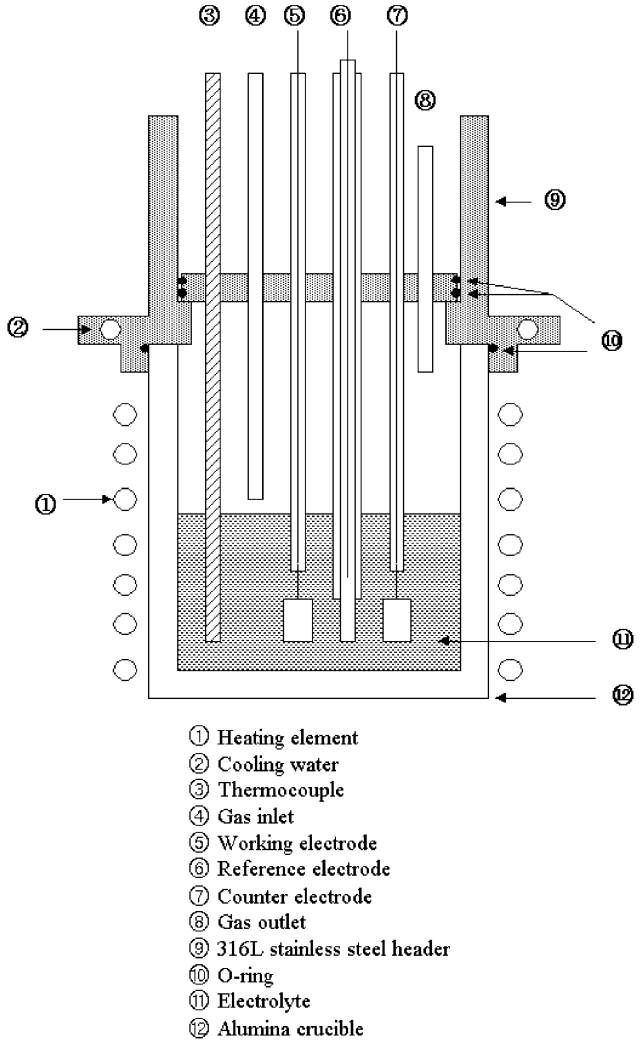

Fig. 2. Schematic diagram of pot cell used for electrochemical tests.

capped with a stainless steel header. A gold wire (0.5 mm diameter) enclosed in two concentric alumina tubes and a gold flag (30 mm × 10 mm × 0.5 mm) were used, respectively, as the reference electrode and the counter electrode. The counter electrode as well as the working electrode was spot-welded to a gold wire. The reference gas consisted of 67% CO_2 and 33% O_2. The same gas was also fed to the melt (area of working electrode) through the inlet for the test in the cathode environment. For the test in the anode environment, a mixture of 80% H_2 and 20% CO_2 was used. Potentiodynamic tests were carried out at a scan rate of 0.1 mV s^{-1} in the potential range −1400 to 400 mV and potentiostatic tests were performed at the equilibrium MCFC anode potential of −1.0 V for 24 h. The Tafel experiment was conducted to estimate the corrosion rate of each specimen, also at a scan rate of 0.1 mV s^{-1} over a potential range in the vicinity of its corrosion potential. All the electrochemical measurements were made by means of a potentiostat/galvanostat (EG&G 263A) controlled by an IBM personal computer with M352 software. The corrosion rate was estimated by PARC calculation in the software.

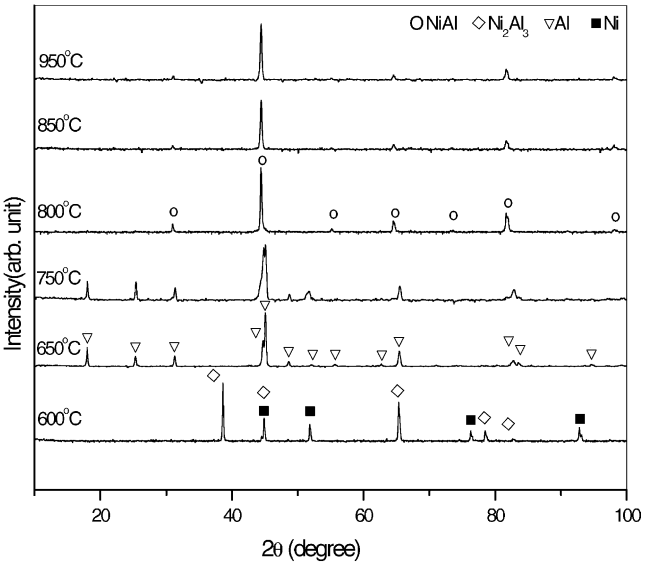

Fig. 3. XRD patterns of Ni–Al electroplated 316L stainless steel heat-treated at various temperatures for 1 h.

3. Results and discussion

3.1. Phases of surface layers

The XRD patterns of a Ni–Al electroplated 316L SS plate heat-treated at various temperatures in the range 600–950 °C are shown in Fig. 3. At 600 °C, which is below the melting point of Al (T_m^{Al}), only elemental phases of Ni and Al can be identified in the pattern. The temperature of 600 °C is probably a little too low for Al and Ni atoms to diffuse far enough and react with each other to form intermetallic compounds. When the temperature rose to 650 °C, still below but close to T_m^{Al}, the increased diffusivity of Al atoms could make the above reaction possible, and indeed a single phase of Ni_2Al_3 has been formed. At 750 °C, a NiAl phase as well as the Ni_2Al_3 phase is present, though close examination is necessary to find the peaks for the NiAl phase. At 800 °C and higher temperatures up to 950 °C, a single phase of NiAl is formed. Kawabata et al. [10] performed a similar experiment using a 310S substrate instead of 316L. They did not present XRD data for surface layers but, according to a schematic diagram illustrating the cross-sectional structure of a specimen, they seemed to observe a surface layer of Ni_2Al_3 and another layer of NiAl underneath when they heat-treated the specimen at 750 °C for 1 h.

Cross-sectional SEM images of specimens heat-treated at 650 and 800 °C are presented in Fig. 4. A surface layer is clearly seen in each of the images. The composition was analysed for each specimen at two points A and B, which represent the inner and outer parts of the surface layer, respectively. This was achieved with energy-dispersive X-ray spectrometry and the atomic ratio of Al/Ni at each

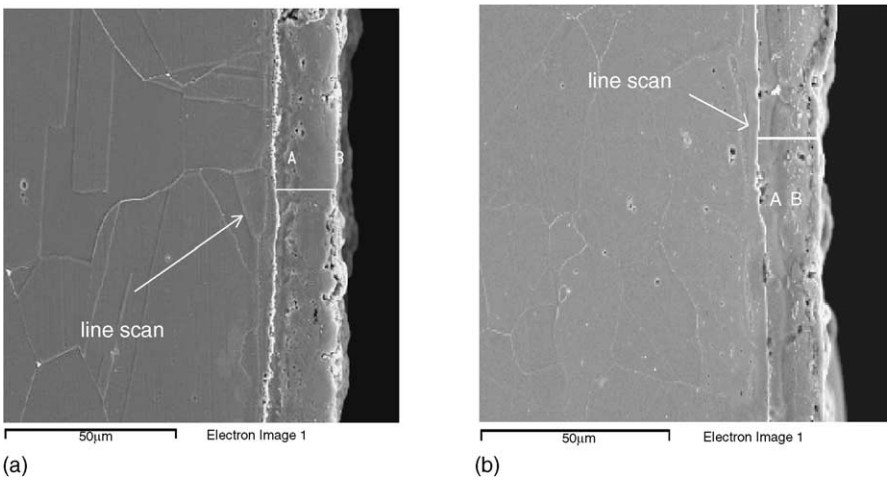

Fig. 4. Cross-sectional electron micrographs of Ni–Al electroplated 316L SS plate heat-treated at (a) 650 °C and (b) 800 °C.

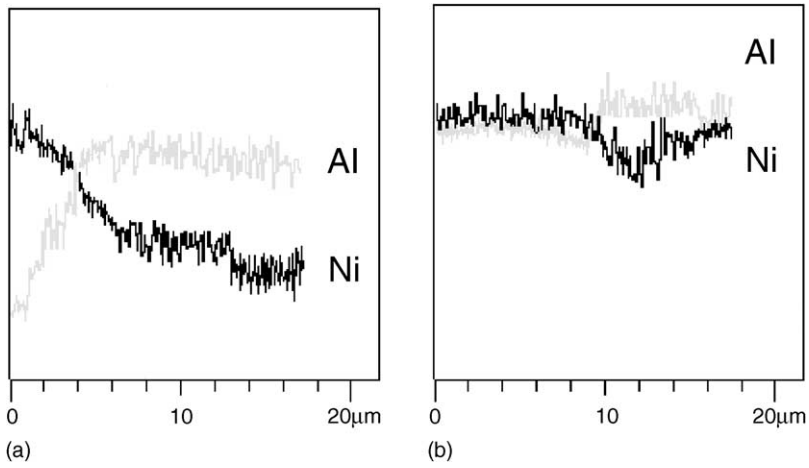

Fig. 5. Intensity profiles of Ni Kα and Al Kα fluorescent X-rays obtained from scan along line marked in Fig. 4 for surface layer of Ni–Al electroplated 316L SS plate heat-treated at (a) 650 °C and (b) 800 °C.

point was estimated from the results. For the specimen heat-treated at 800 °C, the ratio is 0.99 at point A and 1.03 at point B, thus, close to the value of 1 for NiAl. These values together with the intensity profiles of Ni Kα and Al Kα fluorescent X-rays obtained from a scan along the line marked in Fig. 4(b), and shown in Fig. 5(b), confirm that the surface layer of this specimen is composed of the NiAl phase regardless of the position. For the specimen heat-treated at 650 °C, on the other hand, the ratios are 1.16 and 1.53 at points A and B, respectively, and are thus, different from each other. The ratio at point B is close to the value of 1.5 for Ni_2Al_3, and therefore, there is no doubt that the outer part of the surface layer is composed of the Ni_2Al_3 phase. This does not, however, appear to be the case for the inner part since the ratio deviates markedly from 1.5. The reason for this can be found in Fig. 5(a) where line scan results are presented as in Fig. 5(b). According to the data in Fig. 5(a), the surface layer is composed of Ni_2Al_3 phase up to a depth of ∼12 μm, but a phase much richer in Ni than Ni_2Al_3 exists further inside. This phenomenon can be explained by extension of the situation encountered in the work of Colgan et al. [11]. These workers reported that, when double layers of Ni and Al were heated, initially $NiAl_3$ was formed at the interface at around 300 °C, and then Ni_2Al_3 by the reaction of $NiAl_3$ with Ni until all the $NiAl_3$ phase was consumed. Now suppose that some of the Ni phase is left over after the reaction. Then, a phase much richer in Ni than Ni_2Al_3 may be formed at the interface of Ni|Ni_2Al_3 by the reaction of

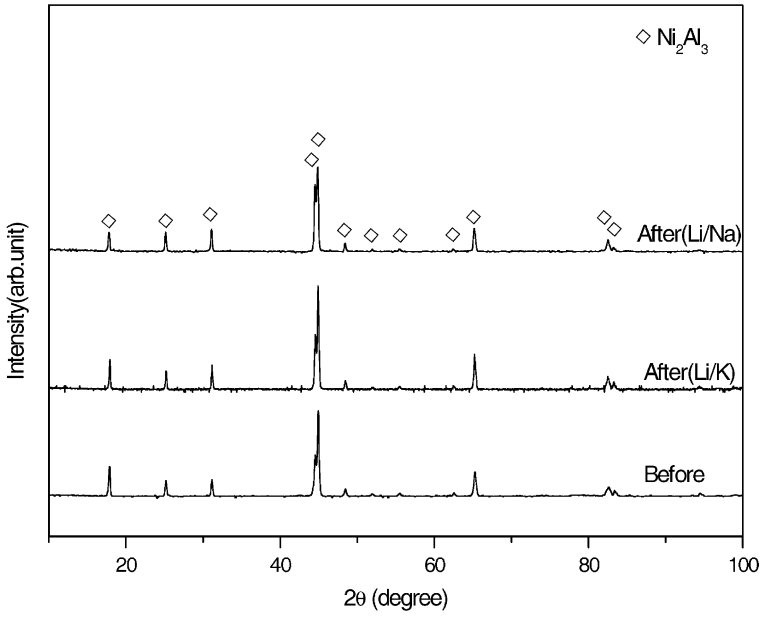

Fig. 6. XRD patterns of Ni_2A1_3–316L specimen before and after immersion tests performed at 650 °C for 100 h in $(Li_{0.62}K_{0.38})_2CO_3$ and $(Li_{0.52}Na_{0.48})_2CO_3$ electrolytes.

these two phases. This distribution of phases, however, does not affect our goal of investigating the effect of a Ni_2Al_3 surface layer on the corrosion behaviour of 316L SS given that the outer part of the surface layer is composed of the Ni_2Al_3 phase to a significant depth.

Based on the above results, a Ni–Al electroplated 316L SS plate was heat-treated at 650 or 800 °C for 1 h to obtain a respective surface layer of Ni_2Al_3 or NiAl, which, for simplicity, will be referred hereafter as Ni_2Al_3/316L or NiAl/316L, respectively.

3.2. Corrosion behaviour

The XRD patterns of a Ni_2Al_3–316L specimen before and after an immersion test carried out in Li–K and Li–Na electrolytes are given in Fig. 6. Regardless of the electrolyte, the patterns look very much alike before and after the test and any extra peaks for corrosion products are not observed after the test. This means that the specimen has not suffered corrosion in the molten electrolyte, possibly due to the corrosion-protective surface layer of Ni_2Al_3. This situation also applies to a NiAl–316L specimen for which XRD patterns are presented in Fig. 7 in a similar manner as in Fig. 6. As expected from the above discussion of the phase of the surface layer, Kawabata et al. [10] performed an immersion test on the Ni_2Al_3/NiAl/310S specimen under the same experimental conditions as, but for much longer time (14 500 h), those employed in this work. They observed a very thin surface layer of $LiAlO_2$ and a layer of NiAl underneath in the specimen after the test [10]. Thus, these results differ from those presented here and this may be due to a large difference in the two experimental times.

Cross-sectional electron micrographs of a Ni_2Al_3/316L specimen after immersion tests carried out in (a) Li–K and (b) Li–Na electrolytes are shown in Fig. 8. Similar micrographs for a NiAl–316L specimen are presented in Fig. 9. It can be seen that the surface layer of Ni_2Al_3 or NiAl maintains good adhesion to the substrate after the test and there is

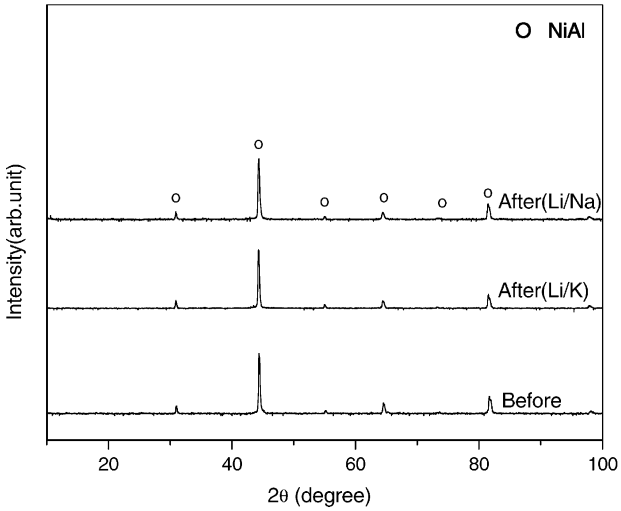

Fig. 7. XRD patterns of NiAl–316L specimen before and after immersion tests performed at 650 °C for 100 h in $(Li_{0.62}K_{0.38})_2CO_3$ and $(Li_{0.52}Na_{0.48})_2CO_3$ electrolytes.

no visible sign of corrosion in either the surface layer or the substrate.

Polarisation curves for bare 316L, Ni_2Al_3–316L and NiAl–316L specimens obtained from potentiodynamic tests performed with a Li–K electrolyte at 650 °C in (a) the cathode environment and (b) the anode environment are given in Fig. 10. In cathode environment, the bare 316L specimen shows the typical polarisation behaviour of an active–passive metal. The corrosion potential is about −1015 mV. As the potential is made more positive, the specimen follows typical Tafel behaviour and the dissolution rate increases exponentially. This is the so-called 'active region'. The maximum anodic current density, which is usually called the critical anodic current density for passivity I_c, appears at about −650 mV where passivation begins. At this potential, the dissolution rate decreases to a very small value and then remains essentially independent of potential over a considerable range. Compared with the bare 316L

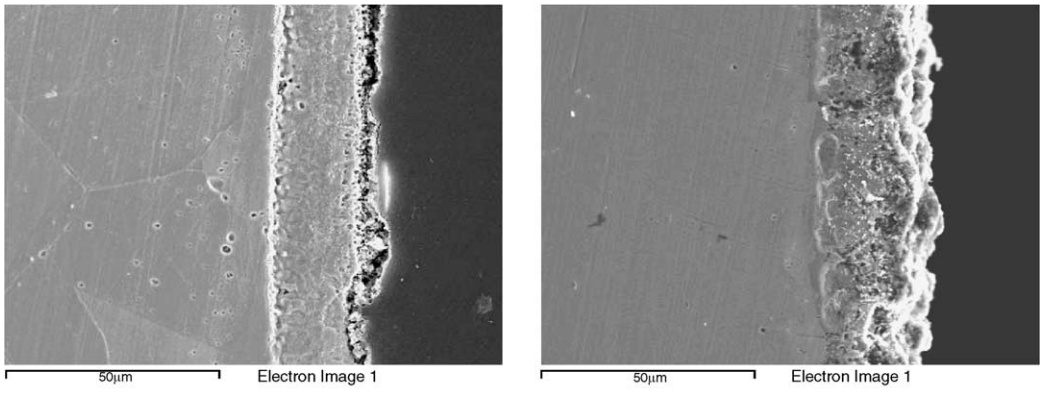

Fig. 8. Cross-sectional electron micrographs of Ni_2Al_3–316L specimen after immersion test performed at 650 °C for 100 h in (a) $(Li_{0.62}K_{0.38})_2CO_3$ and (b) $(Li_{0.52}Na_{0.48})_2CO_3$ electrolytes.

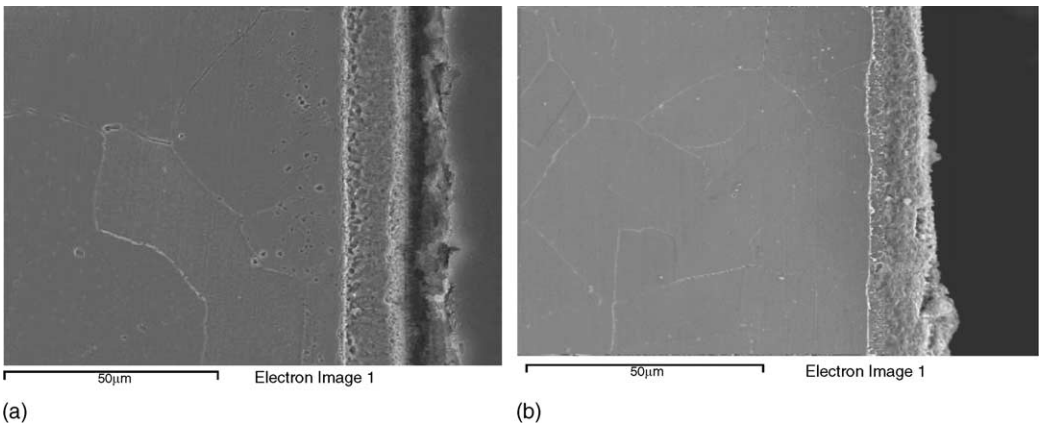

Fig. 9. Cross-sectional electron micrographs of NiAl–316L specimen after immersion test performed at 650 °C for 100 h in (a) $(Li_{0.62}K_{0.38})_2CO_3$ and (b) $(Li_{0.52}Na_{0.48})_2CO_3$ electrolytes.

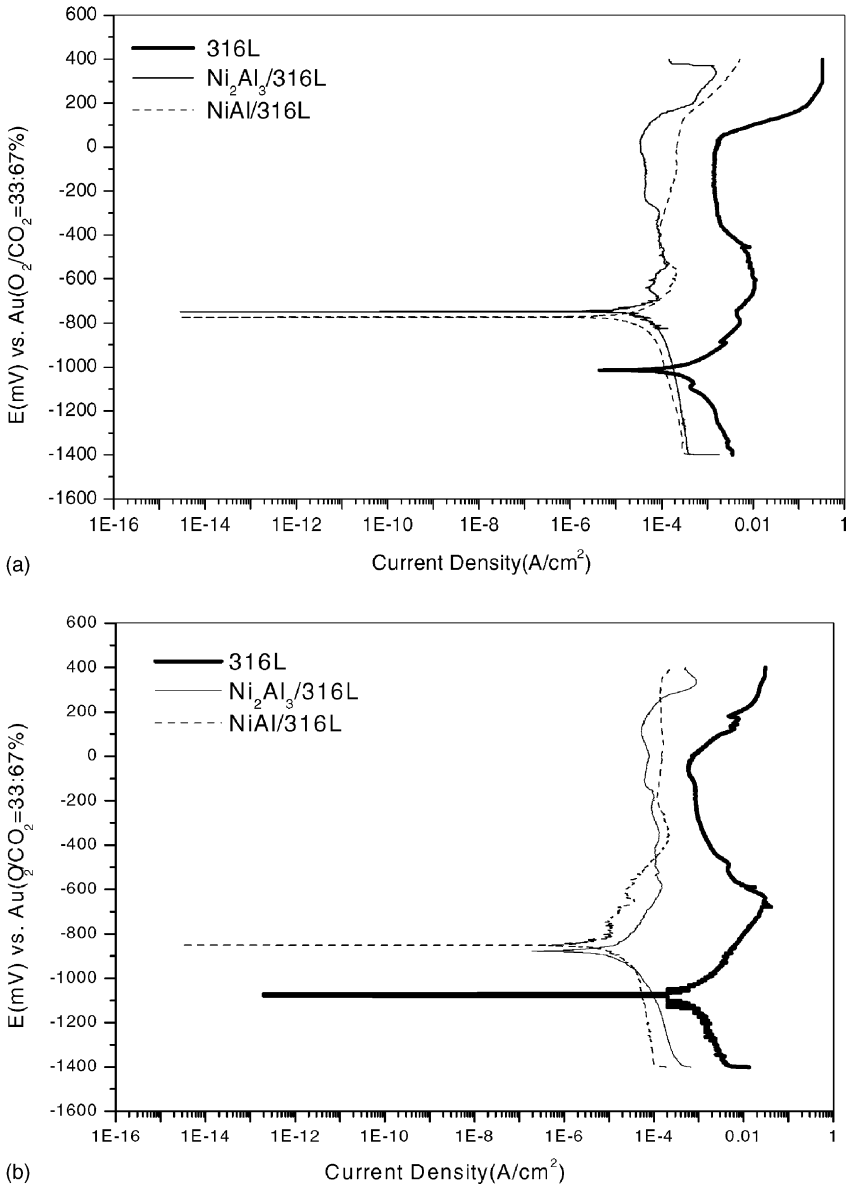

Fig. 10. Potentiodynamic polarisation curves of bare 316L, Ni_2Al_3–316L and NiAl–316L specimens obtained in $(Li_{0.62}K_{0.38})_2CO_3$ electrolyte at 650 °C in (a) cathode environment (O_2/CO_2 = 33%/67%) and (b) anode environment (H_2/CO_2 = 80%/20%).

specimen, a Ni_2Al_3–316L or NiAl–316L specimen shows different polarisation behaviour. For example, the corrosion potentials shift to the anodic side compared with that of a bare 316L specimen. The values are −750 and −770 mV, respectively, for Ni_2Al_3–316L and NiAl–316L specimens. It is well known that corrosion occurs only if the actual electrode potential is more positive than the corrosion potential, and the corrosion rate depends on the difference between the two potentials. Therefore, the shift of corrosion potential to the anodic side observed for the specimens with a surface layer implies a more sluggish occurrence of corrosion, i.e. a higher corrosion resistance, with these specimens than with the bare 316L specimen. Another difference is that the passive current is lower than that for a bare 316L specimen. This is another indication of higher corrosion resistance in the specimens with a surface layer than in the bare 316L specimen, since a smaller magnitude of passive current indicates more readiness of passivation.

In MCFCs, typical electrode potentials are about −50 mV for the cathode and about −1.0 V for the anode [1]. Therefore, it is expected that corrosion will occur with a higher degree of severity on the anode side than on the cathode side. Lee et al. [12] investigated corrosion behaviour of sensitised AISI-type 316L stainless steel in Li–K electrolyte in both the cathode and the anode environment [12]. It was found that the corrosion potential in the anode environment shifted to

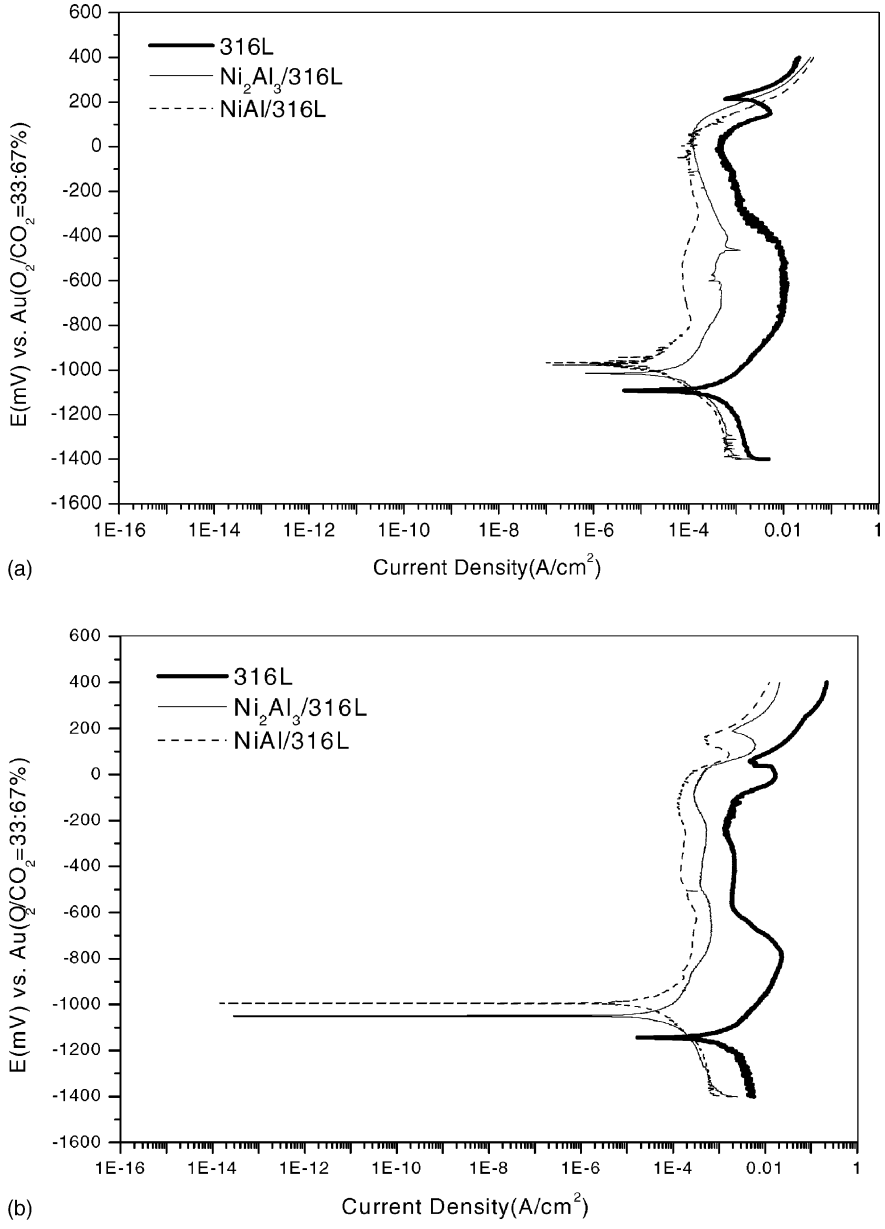

Fig. 11. Potentiodynamic polarisation curves of bare 316L, Ni_2Al_3–316L and NiAl–316L specimens obtained in $(Li_{0.52}Na_{0.48})_2CO_3$ electrolyte at 650 °C in (a) cathode environment (O_2/CO_2 = 33%/67%) and (b) anode environment (H_2/CO_2 = 80%/20%).

the active side by about 100 mV compared with that measured in the cathode environment. Indeed, a comparison of the data in Fig. 10(a) and (b) shows that corrosion potentials measured in the anode environment have shifted to the active side compared with those measured in cathode environment, for example, −1015 to −1075, −750 to −880 and −770 to −840 mV, respectively, for bare 316L, Ni_2Al_3–316L and NiAl–316L specimens. Yet, the value of the passive current for the Ni_2Al_3–316L or NiAl–316L specimen is also lower than that for the bare 316L specimen in the anode environment. Thus, it is concluded that the surface layer of Ni_2Al_3 or NiAl will protect the 316L SS plate from severe corrosion in the Li–K electrolyte, regardless of the environment.

Corrosion is expected to occur more severely in Li–Na electrolyte than in Li–K electrolyte because an oxide scale of Fe_3O_4 or $LiFe_5O_8$, too porous to be corrosion-protective, is formed during cell operation in the forever electrolyte, rather than a dense oxide scale of $LiFeO_2$ usually formed in the latter electrolyte [8]. This expectation can be seen to be realised when Fig. 11, which presents the polarisation curves for the Li–Na electrolyte, is compared with Fig. 10. The corrosion potentials of all the specimens have shifted to the active side compared with corresponding values for the Li–K electrolyte. A part from this behaviour, all the comments made on polarisation curves for the Li–K electrolyte are also applicable to those for the Li–Na electrolyte. Thus, the corrosion potentials measured in the cathode environment shift to the anodic side with respect to the corresponding values for the anode environment, for example, −1093 to −1143, −1014 to −1048 and −970 to −995 mV, respectively, for bare 316L, Ni_2Al_3–316L and NiAl–316L specimens. The corrosion potentials of the specimens with a surface layer appear at more positive values than that of a

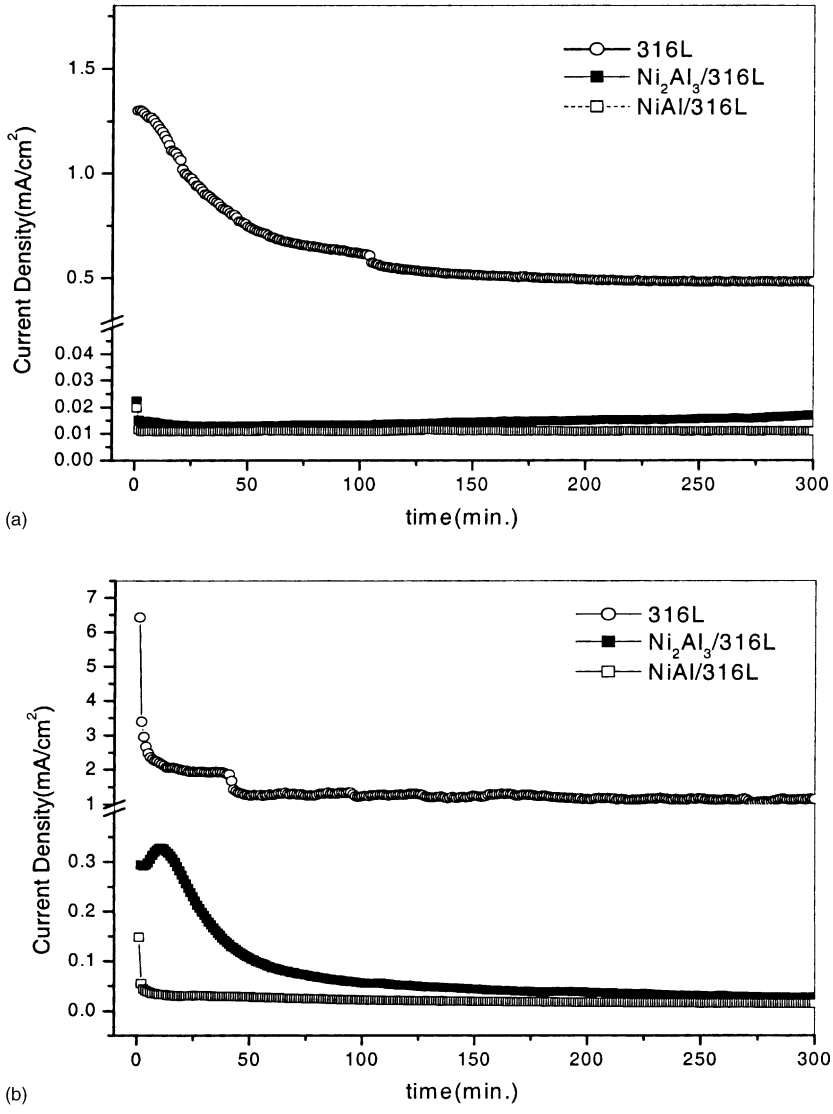

Fig. 12. Potentiostatic polarisation curves of bare 316L, Ni_2Al_3–316L and NiAl–316L specimens obtained at −200 mV in (a) cathode environment (O_2/CO_2 = 33%/67%) and (b) anode environment (H_2/CO_2 = 80%/20%) for $(Li_{0.62}K_{0.38})_2CO_3$ electrolyte at 650° C.

bare 316L specimen. Also, the passive current is lower for the specimens with a surface layer than that for a bare 316L, specimen regardless of the environment. Thus, it can be concluded that the surface layer of Ni_2Al_3 or NiAl greatly enhance the corrosion resistance of 316L SS, regardless of the type of electrolyte or environment.

Potentiostatic tests were performed for another evaluation of the corrosion resistance of the specimens with a surface layer; the results are given in Figs. 12 and 13. The potentiostatic curves for bare 316L, Ni_2Al_3–316L and NiAl–316L specimens obtained in the Li/K electrolyte at 650 °C in cathodic and anodic environments are presented in Fig. 12, and the corresponding curves for the Li–Na electrolyte are given in Fig. 13. The specimens with a surface layer show much lower anodic current densities than a bare 316L specimen in both electrolytes.

The corrosion rates of bare 316L, Ni_2Al_3–316L and NiAl–316L specimens are shown in Fig. 14. In general, the corrosion rates of the specimens are higher in the Li–Na electrolyte or in the anode environment than in the Li–K electrolyte or in the cathode environment, respectively. The estimated value of the corrosion rate is in the range 45.2–74.8 mpy for a bare 316L specimen depending on the electrolyte and the environment. The range is 6.98–17.05 mpy for a Ni_2Al_3/316L specimen and 4.5–7.39 mpy for a NiAl–316L specimen. Hwang and Kang [13] examined the corrosion resistance of the Ni–Al intermetallic compounds. $NiAl_3$, Ni_2Al_3, NiAl, Ni_3Al, prepared by arc-melting, in Li–K electrolyte at 650 °C for 100 h by means of an immersion test [13]. Among the intermetallic compounds, NiAl was the most corrosion-resistant material and Ni_2Al_3 was the second, which agrees with our results.

Thus, based on the data in Figs. 12–14, the specimens with a surface layer have considerably low corrosion rates compared with the bare specimen. Further, for the two surface layers, the corrosion rate of NiAl is a little lower than that of Ni_2Al_3.

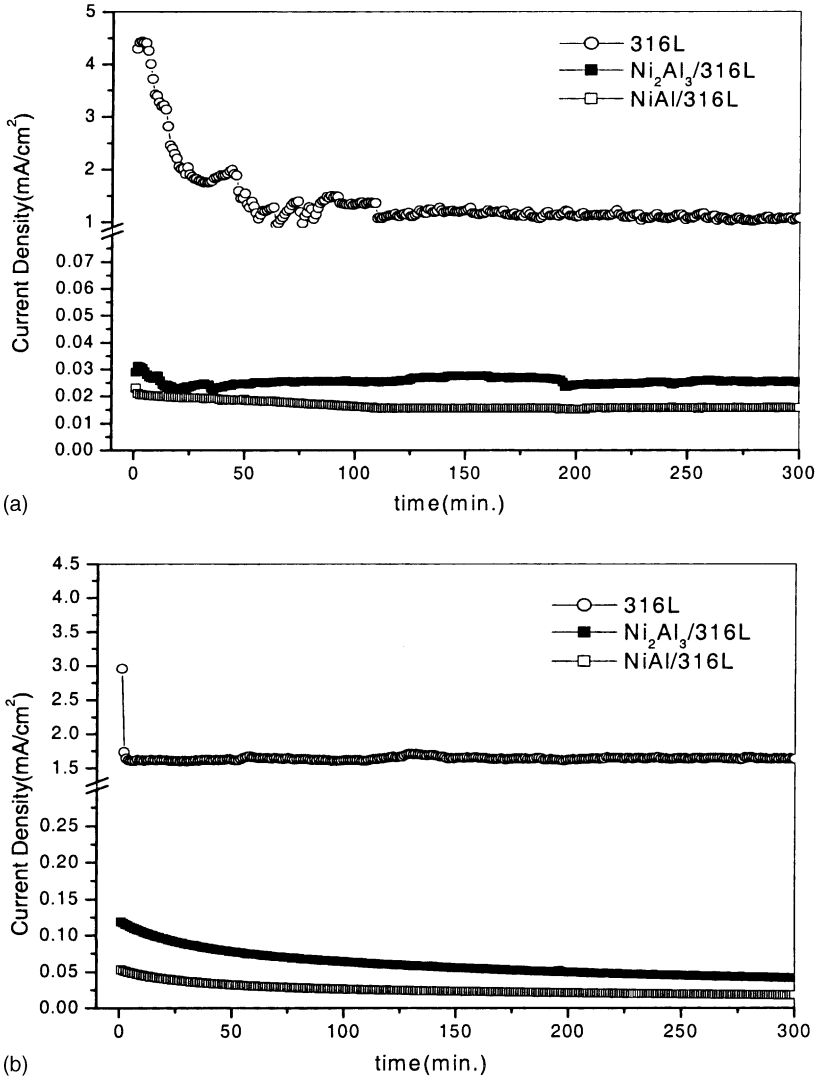

Fig. 13. Potentiostatic polarisation curves of bare 316L, Ni_2Al_3–316L and NiAl–316L specimens obtained at −200 mV in (a) cathode environment (O_2/CO_2 = 33%/67%) and (b) anode environment (H_2/CO_2 = 80%/20%) for $(Li_{0.52}Na_{0.48})_2CO_3$ electrolyte at 650 °C.

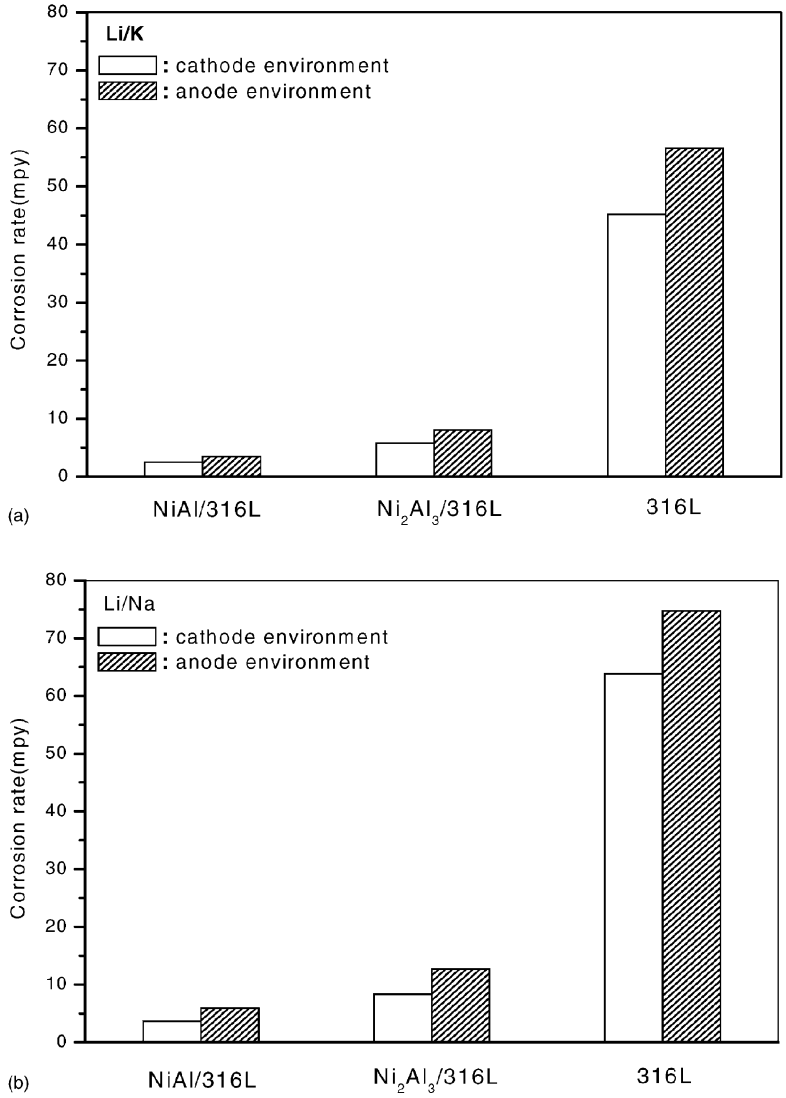

Fig. 14. Corrosion rates of bare 316L, Ni_2Al_3–316L and NiAl–316L specimens estimated for (a) $(Li_{0.62}K_{0.38})_2CO_3$ and (b) $(Li_{0.52}Na_{0.48})_2CO_3$ electrolytes.

4. Conclusions

A 316L SS plate with a surface layer of Ni_2Al_3 or NiAl is prepared by electroplating of elemental metals and subsequent heat-treatment. The corrosion behaviour of each plate is investigated through immersion tests and polarisation measurements and the following conclusions are reached.

1. A surface layer of Ni_2Al_3 or NiAl phase is formed on the 316L SS plate after heat-treatment at 650 or 800 °C, respectively.
2. The surface layer of Ni_2Al_3 or NiAl has good adhesion to the 316L SS plate and protects the plate from corrosion during an immersion test at 650 °C for 100 h in both Li–K and Li–Na electrolytes.
3. The corrosion potentials of specimens with a surface layer shift to more positive values compared with that of a bare 316L specimen, and the passive current of specimens with a surface layer is lower than that of a bare 316L specimen, regardless of the electrolyte or environment.
4. Specimens with a surface layer exhibit considerably low corrosion rates compared with the bare 316L specimen, and the corrosion rate of NiAl is slightly lower than that of Ni_2Al_3.

Acknowledgements

This work was supported by Korea Research Foundation Grant (KRF-99-042-E00075 E3107).

References

[1] R.A. Donado, L.G. Marianowski, H.C. Maru, J.R. Selman, J. Electrochem. Soc. 131 (1984) 2535–2540.
[2] H.S. Hsu, J.H. De Van, M. Howell, J. Electrochem. Soc. 134 (1987) 3038–3043.

[3] J.P.T. Vossen, L. Plomp, J.H.W. de Wit, J. Electrochem. Soc. 141 (1994) 3040–3049.
[4] J.P.T. Vossen, A.H.H. Janssen, J.H.W. de Wit, J. Electrochem. Soc. 143 (1996) 58–66.
[5] J.P.T. Vossen, R.C. Makkus, J.H.W. de Wit, J. Electrochem. Soc. 143 (1996) 66–73.
[6] P. Biedenkopf, M. Spiegel, H.J. Grabke, Electrochim. Acta 44 (1998) 683–692.
[7] J.P.T. Vossen, L. Plomp, J.H.W. de Wit, G. Rietveld, J. Electrochem. Soc. 142 (1995) 3327–3335.
[8] T.H. Lim, E.R. Hwang, H.Y. Ha, S.W. Nam, I.H. Oh, S.A. Hong, J. Power Sources 89 (2000) 1–6.
[9] E.A. Abd El Meguid, Mater. Trans. JIM 38 (1997) 731–736.
[10] Y. Kawabata, N. Fujimoto, M. Yamamoto, T. Nagoya, M. Nishida, J. Power Sources 86 (2000) 324–328.
[11] E.G. Colgan, M. Nastasi, J.W. Mayer, J. Appl. Phys. 58 (1985) 4125–4129.
[12] K.S. Lee, K. Cho, T.H. Lim, S. Hong, H. Kim, J. Power Sources 83 (1999) 32–40.
[13] E.R. Hwang, S.G. Kang, J. Power Sources 76 (1998) 48–53.